MD Simulation of the Na^+−Phenylalanine Complex in Water: Competition between Cation−π Interaction and Aqueous Solvation

Francesca Costanzo and Raffaele Guido Della Valle*

Dipartimento di Chimica Fisica ed Inorganica, Università di Bologna, viale Risorgimento 4, I-40137 Bologna, Italy

Vincenzo Barone

Dipartimento di Chimica, Università Federico II, Complesso Universitario Monte S. Angelo, via Cintia, I-80126 Napoli, Italy

Received: September 16, 2005

The competition between cation−π interaction and aqueous solvation for the Na^+ ion has been investigated by molecular dynamics simulations, using the phenylalanine amino acid as the test π system. Starting from one of the best standard force fields, we have developed new parameters that significantly improve the agreement with experimental and high quality quantum mechanical results for the complexes of Na^+ with phenylalanine, benzene, and water. The modified force field performs very well in forecasting energy and geometry of cation coordination for the complexes. Next, analysis of MD trajectories and steered MD simulations indicate that the Na^+−phenylalanine complex survives for a significant time in aqueous solution and that the free energy barrier opposing dissociation of the complex is sizable. Finally, we analyze the role of different intermolecular interactions in determining the preference for cation−π bonding with respect to aqueous solvation. We thus confirm that the Na^+−phenylalanine stabilization energy may overcome the interactions with water.

I. Introduction

The cation−π interaction, extensively discussed in fascinating reviews by Dougherty and co-workers,[1−3] is the binding force between a cation and a π-electron cloud, usually that of an aromatic ring or alkene chain. Experimental and ab initio quantum mechanical (QM) investigations on the binding energy of cation−molecule complexes in the gas phase have shown that the cation−π interaction is one of the strongest non covalent forces.[3] A dramatic example is that of the Na^+ (benzene) complex, which may be considered as the prototypical cation−π complex, where it is found[4−6] that benzene competes with water, a strongly polar ligand, in binding to Na^+.

Cation−π interactions ought to occur in proteins. In fact, three of the 20 natural amino acids commonly found as building blocks of the proteins, namely phenylalanine, tyrosine, and tryptophan, have fully aromatic character and can thus participate in cation−π interactions. Indeed, in the gas phase these aromatic amino acids bind strongly to the alkali metal cations K^+ and Na^+.[7−13] As reported by the reviews,[3,14] it has often been suggested that the cation−π interaction is important in biological systems, representing a relevant driving force in molecular recognition.[1,2] This statement, which is certainly consistent with the binding energies in the gas phase, is supported by an impressive body of structural investigations on proteins that report arrangements and structures suggestive of significant cation−π interactions.[3,15] Remarkably, these interaction sites, frequent in the nonpolar interior of proteins, even appear on protein surfaces, exposed to aqueous solvation.[16,17] Since cations in water are well solvated, a putative binding site must overcome a substantial desolvation penalty to actually pull a cation out of water. This is definitely possible, as elegantly demonstrated for synthetic molecules designed to mimic the binding properties of biological receptors.[3] The structures of these systems show that hydrophobic pockets lined by aromatic π-rings may stably retain alkali metal cations, even in solution.[2,18,19]

Unfortunately, the energetics of the binding in aqueous solution is not well understood, since quantitative measurements are sparse and refer mainly to interactions between amino acids. The few available measurements, summarized in ref 14, confirm that cation−π interactions between aromatic and positively charged side chains of suitable amino acids have a stabilizing role within proteins and at their surfaces.

To investigate the competition between cation−π interaction and full aqueous solvation for a realistic system, we have decided to perform a molecular dynamics (MD) simulation of the complex between Na^+ and phenylalanine (Phe) in aqueous solution. We have selected this particular complex because Na^+ is one of the strongest cation−π binders,[10,11] while phenylalanine, being a monosubstituted benzene, is the simplest aromatic amino acid. Several experimental[7−11] and QM[9−13,20] reference data on the Na^+(Phe) complex in the gas phase are available.

The article is organized as follows. The available potential models and the data on the complexes of sodium with phenylalanine, benzene, and water, are reviewed in section II. Details on the chosen model and on the MD simulation procedures are supplied in section III. Validation and optimization of the potential parameters, together with the results of the MD simulations, are described in section IV. A brief discussion concludes the paper.

II. Theoretical and Experimental Section Background

A. Potential Models for the Cation−π Interactions. MD simulations rest on the choice of a potential model, which necessarily represents a trade off between accuracy and computational efficiency. Since the exploration of long time scales

10.1021/jp055271g CCC: $30.25
Published on Web 11/10/2005

is a key issue for the simulation of solvated systems, pairwise additive intermolecular potential models, which may be evaluated very efficiently, are the preferred choice. Additive models have been actively developed, and careful reviews are available about the models for water,[21] for Na^+ solvated in water,[22] and for the amino acids.[23] Most models combine atom−atom potentials of the Lennard-Jones (LJ) "12−6" form, $V(r) = A/r^{12} - B/r$,[6] with an electrostatic potential represented by *effective* atomic charges which account, in an average sense, for polarization effects.[24] This feature may allow purely additive models to describe systems where nonadditive many body effects are large. Effective charges of satisfactory quality may be obtained with reliable protocols based on QM calculations.[25,26]

Models for the cation−π interactions are less investigated, compared to those for water and the amino acids, and it must be admitted that no fully satisfactory model has been identified yet. Systematic tests[15] of additive potentials by comparison to QM results have identified the AMBER force field[26] as the least unsatisfactory in describing cation−π interactions between pairs of amino acid side chains. AMBER, which is a commercial model specifically developed to describe flexible amino acids in solution,[26] gave good binding energies, although significant problems remained with the distances[15] between the cation and the aromatic carbons. It was suggested[15] that an additional "12−4" potential between the cation and the aromatic carbons, meant to model the cation−π interaction, might reduce these discrepancies. A similar approach was used to model cation−π interactions for toluene in water,[27] this time by adding to AMBER a "12−10" potential for the cation with the aromatic carbons, plus a similar balancing interaction with the water oxygens. The reasonable success of these calculations suggests that simple additive potential functions may provide effective models of cation−π interactions.

One might harbor doubts about this suggestion, since it has been established that a large component of the cation−π interaction energy is due to various nonadditive polarization effects,[28−30] accounting for the strong interaction between the cation and the induced dipole on the aromatic moiety, and for smaller charge-transfer and donor−acceptor effects. However, the large size of these many-body effects is not necessarily relevant from the point of view of an effective (i.e., average) potential model. In fact, it has been shown that electrostatic effects, mainly the interactions between the cation charge and the quadrupole of the aromatic ring, control the geometric features of the cation−π interactions.[3] The dependence of the binding energy upon the species of the alkali metal cation is also well justified by electrostatic considerations.[3] Furthermore, in two analyses, across series of aromatic molecules,[30,31] it was found that essentially 100% of the variation in the total cation−π binding energy ΔH_{tot} for Na^+ is due to variation in the electrostatic component ΔH_{ele} of the binding. The remaining polarization component ΔH_{pol}, although certainly very large, represents an essentially *constant* contribution ($\Delta H_{pol} \approx -12$ kcal/mol) to the binding energy for the various aromatics.[30,31] These observations all justify the success of the additive potential functions.[15,27] Once the electrostatic interactions are described by a realistic set of charges, a suitable Na^+−carbon atom−atom model, reasonably transferable among different aromatics, should be able to describe the residual non-electrostatic component of the cation−π interaction. Since there are six carbons in an aromatic ring, the well depth ϵ of this Na^+−C model should be close to $\Delta H_{pol}/6$, i.e., $\epsilon_{Na^+C} \approx 2$ kcal/mol.

B. Reference Structure of the Na^+(Phe) Complex. As discussed in the Introduction, we aim at simulating a Na^+(Phe) complex solvated in water. Like all other amino acids, phenylalanine in its free acid form carries simultaneously a basic amine function $-NH_2$ and a carboxylic acid function $-COOH$. In aqueous solution the proton of the $-COOH$ group is transferred onto the amine to give a dipolar, but still globally neutral, zwitterionic (ZW) form, with $-COO^-$ and $-NH_3^+$ ends.[33] The Na^+(Phe) complexes in absence of the solvent have been extensively studied.[7−13] As indicated by the theoretical calculations,[9−13] the complex is most stable in a free acid configuration. As theoretically shown by Siu and Ma[13,20] the complex may also assume stable zwitterionic configurations. In fact, interactions with the Na^+ cation may stabilize the $-COO^-$ end of the zwitterionic form. Two different stable zwitterionic configurations are predicted,[13,20] called ZW5 and ZW3. The ZW5 configuration, shown in Figure 1, presents interactions of interest for our study. In this structure, in fact, the Na^+ cation interacts simultaneously with the phenyl (π electrons) and carboxylate ($-COO^-$) groups. Cation−π interactions are missing in the ZW3 configuration.[13,20] Since solvated amino acids are preferentially in zwitterionic form, and because only the ZW5 conformation presents cation−π interactions, we have chosen this form, among all predicted structures of the complex,[13,20] for our calculations.

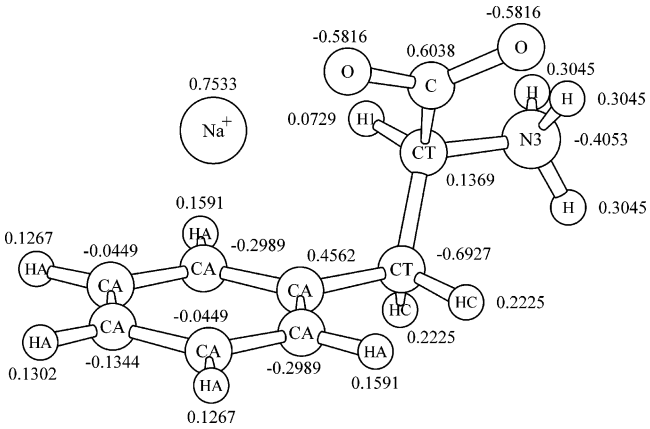

Figure 1. Structure of the Na^+(Phe) complex in the ZW5 zwitterionic conformation.[13] Atoms are labeled by their AMBER types,[26] with ESP charges indicated nearby. Chemically equivalent atoms have identical charges, obtained by averaging their initial ESP charges. Graphics by MOLSCRIPT.[32]

C. Validation Benchmark. Since there is no well-established model for the cation−π interactions in water, it becomes necessary to validate any candidate potential model. Acceptable models should at least reproduce the geometry and energetics in the gas phase of the complexes Na^+(Phe), $Na^+(C_6H_6)$ and $Na^+(H_2O)_n$ with small n, thus ensuring a stable ZW5 complex, a fair cation−π binding, and a credible representation of the competition with solvation in water. The structures and classical binding energies ΔE_{pot} of the complexes constitute a good benchmark to validate a potential model, since they may be computed very rapidly by minimizing the model potential energy E_{pot}. The prediction of all models will be compared to benchmark data, reported in Table 1, which summarizes the available experimental and QM results.

The experimental benchmark data on the binding energies of the $Na^+(C_6H_6)$ and $Na^+(H_2O)_n$ complexes[4−6] come from high-pressure mass spectrometric (HPMS) equilibrium measurements,[5,6] which yield binding enthalpies ΔH_T at the measurement temperature T, and from threshold collision-induced dissociation (CID) experiments,[4] which yield true 0 K dissociation enthalpies ΔH_0. The experimental results are in agreement with the abundant literature on the QM binding enthalpies of

TABLE 1: Binding Energies (kcal/mol) and Interatomic Distances (Å) for the Complexes Na^+(Phe), $Na^+(C_6H_6)$, $Na^+(H_2O)_n$ with n up to 6, and for Na^+ in Aqueous Solution[a]

system	configuration		AMBER	model	QM	ref	expt.	ref
Na^+(Phe)	ZW5	$E_{binding}$	−35.25	−37.69	−37.73	[13]		
		r_{NaO}	2.33	2.14	2.10	[13]		
		$\overline{r_{NaC}}$	5.52	2.99	2.93	[13]		
$Na^+(C_6H_6)$	C_{6v}	$E_{binding}$	−18.66	−25.64	−24.6	[36]	−21.1, −28.0	[4,6]
		r_{NaC}	2.70	2.78	2.77	[36]		
$Na^+(H_2O)$	C_{2v}	$E_{binding}$	−23.33	−22.07	−23.3	[35]	−22.6, −24.0	[4,5]
		r_{NaO}	2.32	2.27	2.21	[35]		
$Na^+(H_2O)_2$	D_{2d}	$E_{binding}$	−45.30	−42.71	−43.1	[35]	−43.8	[5]
		r_{NaO}	2.33	2.28	2.25	[35]		
$Na^+(H_2O)_3$	D_3	$E_{binding}$	−64.68	−60.63	−59.5	[35]	−59.6	[5]
		r_{NaO}	2.34	2.29	2.29	[35]		
$Na^+(H_2O)_4$	S_4	$E_{binding}$	−81.41	−75.75	−73.9	[35]	−73.4	[5]
		r_{NaO}	2.36	2.30	2.31	[35]		
$Na^+(H_2O)_5$	C_2 (4+1)	$E_{binding}$	−94.46	−87.24	−87.7	[35]	−85.7	[5]
		r_{NaO}	2.35	2.30	2.30	[35]		
	C_2 (5)	$E_{binding}$	−93.92	−89.24	−85.3	[35]		
		r_{NaO}	2.39	2.34	2.32	[35]		
$Na^+(H_2O)_6$	D_{2d} (4+2)	$E_{binding}$	−103.14	−94.45	−99.5	[35]	−96.4	[5]
		r_{NaO}	2.35	2.30	2.30	[35]		
	S_6 (6)	$E_{binding}$	−104.54	−99.78	−96.9	[35]		
		r_{NaO}	2.42	2.35	2.42	[35]		
Na^+(water)	solution	r_{NaO}	2.46	2.40	2.49	[37]	2.40, 2.44	[38,39]
		$\overline{r_{NaO}}$	5.76	5.93	5.2	[37]	4.9, 6.0	[38,39]

[a] For Na^+(Phe) we indicate the distance r_{NaO} with the closest O atom in the $-COO^-$ group and the average distance $\overline{r_{NaC}}$ with the C atoms in the phenyl ring. For the other systems we report the unique or the average distances r_{NaC}, r_{NaO} or $\overline{r_{NaO}}$, as appropriate, and the average coordination number $\overline{r_{NaO}}$. Classical binding energies ΔE_{pot} calculated at potential energy minima with the AMBER[26] model and with our modified model are compared to QM binding energies[13,35,36] and to experimental binding enthalpies ΔH_T estimated for $T = 0$,[4] 298[5] and ≈ 600 K.[6] Classical MD results are compared to QM MD[37] and X-ray[38,39] data.

the two complexes, summarized by Hoyau.[34] Among the available QM energies for $Na^+(C_6H_6)$ and $Na^+(H_2O)_n$, we have chosen as benchmark data the large basis sets results by Feller,[35,36] at the MP2 level (including diffuse functions on the lighter atoms). All structural data also come from these calculations,[35,36] since no measurement is available.

For the Na^+(Phe) complex in the gas phase, a recent review[11] reports experimental[7−11] and QM[9−13] binding energies in the ranges 41.5−49.1 and 46.85−48.08 kcal/mol, respectively. Supported by the QM calculations, all authors[7−13] indicate that the most stable complex is formed with the free acid. Only a single QM calculation,[13] without matching measurements, is available as a benchmark for the relatively less stable zwitterionic configuration ZW5. The computed binding energy, −37.73 kcal/mol, is a B3LYP/6311+G(3df,2p) result with zero-point energy corrections,[13] which appears sufficiently reliable since the corresponding result for the free acid form[13] is excellent.[11] The QM geometries[13] are optimized at the B3LYP/6-31G* level.

III. Methods

A. Potential Model and Initial Parameters. For lack of a better choice,[15] we started our calculations using the AMBER model.[26] In this model the intermolecular interactions are mimicked by a two-body atom−atom potential $V_{ij}(r)$ with electrostatic and Lennard-Jones (LJ) terms, $V_{ij}(r) = q_iq_j/r + 4\epsilon_{ij}[(\sigma_{ij}/r)^{12} - (\sigma_{ij}/r)^6]$. The point charges q_i are located on the atoms. In the default model, the "radius" and "energy" parameters σ_{ij} and ϵ_{ij} involving unlike atomic species i and j obey standard mixing rules $\sigma_{ij} = (\sigma_{ii} + \sigma_{jj})/2$ and $\epsilon_{ij} = \sqrt{\epsilon_{ii}\epsilon_{jj}}$. As discussed in section IVB, we have eventually found it necessary to relax the mixing rules.

Short distance intramolecular interactions are represented by a sophisticated model[26] which includes stretchings, bendings, and torsions (labeled 1−2, 1−3, and 1−4 interactions). More distant intramolecular pairs of atoms interact through the usual atom−atom potential, which, after a suitable scaling[25,26] (by 1/1.2 and 1/2 for electrostatic and LJ interactions, respectively) also acts on 1−4 pairs.

The LJ potential parameters for phenylalanine were initially taken from the standard AMBER parameter set,[26] with the atomic types indicated in Figure 1. These atomic types indicate the atomic species and their chemical environment. Together with the molecular topology, they completely identify the parameters of the intramolecular interaction. For water we adopt the charges and the oxygen LJ parameters of the SPC model of Berendsen and co-workers,[24,40] with the modifications introduced by Gervasio[41] and implemented in the ORAC package[42] to allow for a flexible bond angle. The Na^+ cation has the LJ parameters and the formal charge $q_{Na+} = 1$ of the Åqvist model.[43] The Åqvist and SPC models are both well matched to the AMBER parameter set.[26]

Following the AMBER protocol,[26] the remaining atomic charges have been fitted to the QM electrostatic potential (ESP) evaluated at the 6-31G* level. The developers of AMBER justify this choice by noticing that polarization effects in condensed phases tend to increase the average dipole moment over the gas phase. The 6-31G* basis set, which systematically overestimates the gas-phase dipole, may thus yield better effective atomic charges than larger basis sets.[26] The ESP charges for benzene[26] are $q_H = -q_C = 0.145$. The ESP charges for the Na^+(Phe) complex in the ZW5 conformation,[13] obtained at the B3LYP/6-31G* level,[44−46] and averaged over chemically equivalent atoms, are shown in Figure 1. The oxygens of the carboxylate group $-COO^-$ have been considered as equivalent since in preliminary simulations in aqueous solution we have found that the $-COO^-$ moiety rotates.

The ESP charges for Na^+(Phe) appear quite acceptable. In fact, the average charges on the phenyl ring are close to those

for benzene, and those on the $-COO^-$ and $-NH_3^+$ groups are chemically reasonable. The charge of the Na^+ ion, $q_{Na+} = 0.7533$, matches the charge $q_{Na+} = 0.76$ calculated[47] for $Na^+(C_6H_6)$ and indicates a significant charge-transfer effect. For consistency with the Åqvist model used by AMBER,[26] we have initially neglected the charge transfer, maintaining the formal ionic charge $q_{Na+} = 1$. However, since this charge gave unsatisfactory results, we have eventually chosen the ESP charge, as discussed in section IVB.

B. Molecular Dynamics Simulations. As discussed below (sections IVD and IVE), we have first simulated a single Na^+ cation in water and then a Na^+(Phe) complex in water, using the program ORAC.[42] The MD simulations were performed in the *NVT* ensemble (constant number of particles, volume, and temperature) using a Nosé thermostat[48] to maintain the temperature at an average of 300 K. A cubic box was used, with periodic boundary conditions and side length $L = 21.746$ Å. The space not occupied by the Na^+ or Na^+(Phe) solute was filled with SPC water[24,40] with the experimental density[49] of 0.9970 g/cm^3 at 300 K. The chosen box size, which required 341 H_2O molecules for Na^+ and 332 for Na^+(Phe), allows space for at least two and half layers of water around the Na^+(Phe) complex (whose largest dimension is ≈ 8.15 Å).

Electrostatic interactions were calculated using the smooth particle mesh Ewald method (PME),[50] with a screening factor $\alpha = 5.714/L$.[51] The direct space and reciprocal space sums were extended up to spherical cutoffs of $L/2$ and $16 \times 2\pi/L$, respectively. These values were optimized to reduce the series truncation error in the potential energy to less than one part in 10^4 while reducing computer time. The equations of motion were integrated with the r-RESPA algorithm[52,53] developed for protein systems,[54] with a single time step of 2 fs. The C−H, N−H, and O−H bond lengths were held fixed, while all other intramolecular degrees of freedom, including stretchings not involving hydrogen atoms, were explicitly integrated.

C. Free Energy Calculations. To study the binding between Na^+ and phenylalanine in water, we have chosen a reasonable reaction coordinate, namely the distance z between the Na^+ cation and the plane of the phenyl ring, and computed the potential of mean force (PMF) as a function of z. The PMF describes the free energy profile $\Delta F(z)$ along the reaction coordinate z, with all the other degrees of freedom effectively averaged out. To compute the PMF we have followed a steered MD procedure,[55,56] in which the system is pushed along the reaction coordinate by applying a time dependent external potential $U_{steer}(z)$. We have used a simple harmonic potential $U_{steer}(z) = k(z - z_t)^2/2$, where z is the actual reaction coordinate and z_t is the steered coordinate, continuously varying with time t. We have varied z_t at a speed of 4 Å/ns, using a force constant $k \approx 150$ kcal mol^{-1} Å^{-2}, sufficient to maintain the fluctuations of z, $\sigma_z \approx \sqrt{k_B T/k}$, well below 0.1 Å.

The free energy is then computed by thermodynamic integration. Let F_z be the free energy of the system in contact with the heat bath and described by the classical Hamiltonian H_z, where the reaction coordinate z is considered as a controllable external parameter. Starting from an initial state, with $z = z_0$ and free energy F_{z0}, a change in z results in a variation of the free energy, $\Delta F(z) = F_z - F_{z0}$, and in work performed on the system, $W_{z0\rightarrow z} = \int_{z_0}^{z} \langle H_z/\partial z \rangle_z \, dz$. Here $\langle \cdots \rangle_z$ indicates the canonical average in the state described by H_z. The expended work normally exceeds the free energy gain, $W_{z0\rightarrow z} \geq \Delta F(z)$. The difference between the two quantities vanishes in the limit of a sufficiently slow change of z, where the work becomes reversible and may be used as an estimate of the PMF, $\Delta F(z) \approx W_{z0\rightarrow z}$.

In practice, this PMF estimate is affected by two sources of uncertainty, one arising from the many alternative paths that the system may choose during the steering, and another due to the irreversibility of the work when the trajectory is followed at nonzero speed. We have disentangled the two sources of uncertainty by sampling a number of different paths and by reversing the steering direction, as discussed in section IVE, and found that the uncertainty due to irreversibility is the less important one. The method due to Jarzynski,[57] which eliminates the consequences of irreversibility at the cost of increased sampling uncertainty,[58] is thus not convenient in our case.

IV. Results and Discussion

A. Test of the Initial Parameters. To validate the initial AMBER parameters, and as discussed in section IIC, we have calculated the structures of minimum potential energy for the complexes Na^+(Phe), $Na^+(C_6H_6)$, and $Na^+(H_2O)_n$, with n up to 6. The results, reported in Table 1, are quite disappointing. The Na^+(Phe) complex predicted by AMBER, although with a binding energy close to the QM benchmark,[13] does not reproduce the correct ZW5 conformation.[13] In fact, the average distance $\overline{r_{NaC}}$ between the Na^+ cation and the C atoms in the phenyl ring is much larger than the QM value,[13] showing that the cation$-\pi$ interaction is not well reproduced. Perhaps of minor concern, the distance r_{NaO} with the closest O atom in the $-COO^-$ group is too large. Also for the benzene complex, there are serious problems with the cation$-\pi$ interaction, since $Na^+-C_6H_6$ is less bound than Na^+-H_2O, at variance with the experimental and QM data.[4,6,34,36] The results for the $Na^+-(H_2O)_n$ clusters are more satisfactory, especially for the smaller clusters. For the larger clusters, as already noticed in previous investigations on the Åqvist's model for $Na^+-(H_2O)_n$ clusters,[59] the computed binding energies tend to become too negative in comparison to the experimental and QM data.[4,5,35]

All aspects of the AMBER model probed by the benchmark present problems: the interactions of the Na^+ cation with the aromatic carbons of benzene or phenylalanine (labeled CA carbons in the AMBER force field), those with the O atoms in the $-COO^-$ group (labeled O) and, to a lower extent, those with the oxygens in the water molecule (which we label O′). In light of the mixed results reported by the previous calculations[15,27] on cation$-\pi$ interactions using the AMBER model, the presence of defects in the Na^+-CA, Na^+-O, and Na^+-O′ potentials was probably to be expected.

B. Optimization of the Potential Model. Since the AMBER potential is not satisfactory, we have decided to improve it, especially for what concerns the cation$-\pi$ interaction between Na^+ and the aromatic carbons. Instead of introducing additional "12−4" or "12−10" interactions,[15,27] and following the suggestion of Caldwell,[28] we prefer to relax the "mixing rules" for the interactions Na^+-CA, Na^+-O and Na^+-O′, retaining the standard "12−6" potential. All other LJ interactions are left unchanged with their original AMBER parameters.[26] In several attempts using the formal charge $q_{Na+} = 1$, with various schemes for allocating the total charge of the phenylalanine molecule, it proved impossible to reproduce simultaneously the binding energies of both Na^+(Phe) and $Na^+(C_6H_6)$. As discussed in section IIA, a Na^+(carbon) potential transferable among different aromatics requires a realistic charge model for the electrostatic component ΔH_{ele} of the cation$-\pi$ interaction. For this reason, we have finally decided to replace the Åqvist charge with the ESP charge derived from the electrostatic potential (Figure 1), thus accounting for the average of the charge-transfer effects. Of course, this implies an altered description of the electrostatic

TABLE 2: Optimized ϵ_{ij} (kcal/mol) and σ_{ij} (Å) Lennard-Jones Parameters between NA^+ and sp^2 Aromatic Carbons (CA), Carboxylic Group Oxygens (O), and Water Oxygens (O′) (potential minima occur at $r_{ij}^{min} = 2^{1/6}\sigma_{ij}$)

ij	ϵ_{ij}	σ_{ij}	r_{ij}^{min}
NA^+-CA	1.770	2.570	2.885
NA^+-O	1.620	2.056	2.308
NA^+-O'	2.237	2.233	2.506

interaction with water, which must be balanced by modifying the atom−atom LJ parameters. The LJ parameters were adjusted by aiming for a semiquantitative agreement between the predictions of the model and the benchmark data on the complexes Na^+(Phe), $Na^+(C_6H_6)$, and $Na^+(H_2O)_n$. The adjustment was quite straightforward, thanks to the obvious hierarchy present in the model. In fact, the results for the $Na^+(H_2O)_n$ complexes are affected only by the Na^+-O' parameters, and those for $Na^+(C_6H_6)$ only by the Na^+(CA) parameters. These latter parameters, together with the Na^+(O) ones, influence the results for Na^+(Phe).

The potential parameters finally chosen to represent the complexes are listed in Table 2. The choice of this particular model is to some extent arbitrary, because similar results can be reached with many alternative models due to the large correlation among the parameters, and because the selection of the benchmark data used in the fit is also arbitrary. No particular meaning should be ascribed to the potential parameters, which are simply tools used to describe the interactions. Nevertheless, it is reassuring to find that the potential depth ϵ_{Na+CA} is close to the expected value of 2 kcal/mol, and that the QM[13,35,36] and X-ray[38,39] interatomic distances r_{ij} (Table 1) lie in the deep region of the model potential, between the zero and the minimum of the LJ potential, $r_{ij}^0 = \sigma_{ij}$ and $r_{ij}^{min} = 2^{1/6}\sigma_{ij}$, respectively (Table 2).

The potential model, with the chosen ESP charges, is designed to describe the competing Na^+(Phe) and $Na^+(H_2O)_n$ conformations on which it has been calibrated. Modifications in the charge transfer, which might be relevant during the transition between the two types of conformation, are not representable with constant charges. These dynamical effects have been explored for several test systems by determining the ESP charges on-the-fly during mixed quantum mechanics−molecular mechanics (QM−MM) simulations.[60] The effects are probably small in our case, since for a zwitterionic dipeptide in aqueous solution[60] the test system closest to our target system, constant AMBER point charges, and dynamical ESP charges (D-RESP) were found to be consistent.

C. Minimum Energy Structures of the Na^+ Complexes. As a first test of the modified potential model, we have determined the structures of minimum potential energy for the various Na^+ complexes. Binding energies and interatomic distances are reported in Table 1, while most structures are drawn in Figure 2. As shown by Table 1, the present potential model yields correct binding energies for both Na^+(Phe) and $Na^+(C_6H_6)$, together with Na^+-C and Na^+-O distances in excellent agreement with the QM results.[13,36] Since fitting these energies and distances was the primary reason for relaxing the mixing rules, such a result can be considered fully satisfactory.

The computed structures of the $Na^+(H_2O)_n$ complexes, drawn in Figure 2, match the corresponding QM structures.[35] Indeed, Table 1 shows that the energies and distances computed with the present model are even better than those computed with the original AMBER model,[26] thus indicating that the changes in the electrostatic interactions between Na^+ and water have been satisfactorily balanced by the modified atom−atom model.

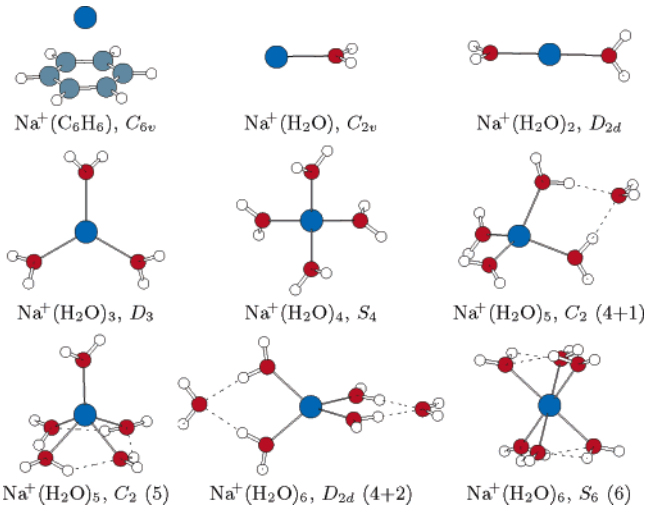

Figure 2. Minimum energy structures of $Na^+(C_6H_6)$ and $Na^+(H_2O)_n$ complexes, labeled by their symmetry group and, for $n \geq 5$, by their coordination around the Na^+ cation. Solid and broken lines indicate Na^+-O and H−O hydrogen bonds, respectively. Orientation and labeling match those of refs 35, 36.

An acceptable balancing is important, because the structure of the $Na^+(H_2O)_n$ complexes is controlled by the competition between the Na^+-O attraction, which favors high-symmetry structures where all H_2O molecules are coordinated to the Na^+ cation, and the water−water interactions, which favor the formation of a second coordination shell. When the number of H_2O molecules increases, direct coordination to the cation leads to excessive crowding and becomes progressively less favorable. In fact, the QM calculations[35] indicate that for $n = 5$ or 6 the most stable structures exhibit (4+1) or (4+2) arrangements. These arrangements exhibit a first coordination shell containing four H_2O molecules, linked by H−O hydrogen bonds to one or two H_2O molecules in a second shell. More compact (5) or (6) arrangements, where all H_2O molecules are in the same shell, are slightly less stable.

As previously noticed,[61] the reduction in binding energy for each additional H_2O molecule is driven by the water−water interactions which, to retain compatibility with the AMBER force field,[26] we have not modified. By decomposing the total energy of the $Na^+(H_2O)_n$ complexes into Na^+-H_2O and H_2O-H_2O contributions, we have found that for $n = 2$, 3, or 4 all individual Na^+-H_2O pairs have interaction energies around −22 kcal/mol, essentially coincident with that for a single $Na^+(H_2O)$ dimer (Table 1). The reduced binding is due to the interactions between the water molecules within the solvation shell, which leads to a net repulsive contribution, ≈1.4, 5.2 and 11.6 kcal/mol for $n = 2$, 3, and 4. Excessive crowding, in the larger complexes with $n = 5$ or 6, leads to arrangements with less favorable Na^+-H_2O pair interactions energies, around −16.5 kcal/mol. The present potential model, which does not reproduce the QM energy ordering for the arrangements (4+1), (5), (4+2), and (6), is not yet completely satisfactory. This discrepancy, which could be eliminated by tuning the water−water interactions, is not a cause of serious concern because the energies of the various arrangements remain quite good. However, it must be taken into account that the present potential model, like the AMBER model,[26] probably overestimates the sodium−water coordination.

D. Na^+ in Aqueous Solution. As a further test of the potential model, we have simulated a Na^+ cation in aqueous solution. This test, which allows us to investigate a wide range of Na^+-O distances, is necessary since the modified Na^+ charge might

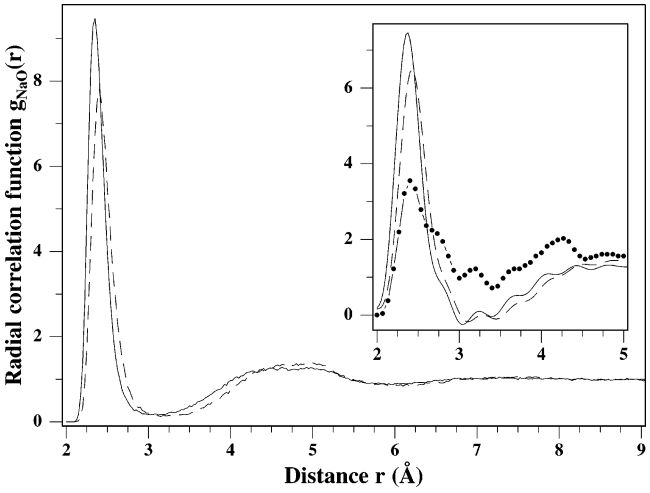

Figure 3. Main graph: pair radial correlation function $g_{NaO}(r)$ for Na^+ in aqueous solution, calculated with the present model (solid line) and with the AMBER model[26] (broken line). Inset: calculated $g_{NaO}(r)$ functions after convolution with the experimental[38] resolution function $H(r)$ (lines), compared to the experimental[38] $g_{NaO}(r)$ (symbols).

alter the long-range interactions. The benchmark data on the $Na^+(H_2O)_n$ complexes, in fact, probe only the Na^+-O ordering in the first two coordination shells. The simulations were performed as described in section IIIB, and involved equilibration for 1 ns or more, followed by data collection for further 0.16 ns.

The effect of the modified potential on the energy is not large. By replacing the AMBER model[26] with the present model, the total potential energy of the simulation box becomes slightly less negative (by at most 6.5 kcal/mol in the equilibrated system). The results for Na^+ in aqueous solution, which may be considered as a huge $Na^+(H_2O)_n$ cluster, thus follow the trend displayed by Table 1 for the larger clusters, where the present model tends to become somewhat less binding than AMBER.[26] Since the energy difference between AMBER and the present model is so small, we have judged unnecessary the evaluation of the two separate solvation energies.

The pair radial correlation functions $g_{NaO}(r)$ computed for the AMBER model and with the present model are shown in Figure 3. The corresponding average neighbor distance $\overline{r_{NaO}}$ and average number $\overline{r_{NaO}}$ of Na^+-O neighbors are reported in Table 1. These parameters have been estimated by integrating the radial correlation function $g_{NaO}(r)$ up to the first minimum, which for both the AMBER and the present models occurs around $r = 2.9$ Å. The exact position of the minimum is largely immaterial, since shifting it by ± 0.1 Å alters $\overline{r_{NaO}}$ by ± 0.1, and $\overline{r_{NaO}}$ by only ± 0.01 Å. The AMBER model and the present one exhibit no differences in the long range order, because at distances beyond the second coordination shell the two computed $g_{NaO}(r)$ functions are featureless and essentially identical. Instead, there are small differences in the first and second coordination shells around the sodium cation, occurring near 2.40 and 4.75 Å, respectively, where the present model favors shorter distances $\overline{r_{NaO}}$ and a higher coordination $\overline{r_{NaO}}$. As shown by Table 1, these differences are consistent with the results for the $Na^+(H_2O)_n$ complexes.

For both models, the average neighbor distance is in agreement with the available QM (Car−Parrinello MD)[37] and X-ray[38,39] data summarized in Table 1, while the coordination is probably a bit too large. To allow for a more detailed comparison, we have convoluted the computed $g_{NaO}(r)$ functions, with the experimental[38] resolution function $H(r)$. The resulting functions, shown in the inset of Figure 3, reproduce very well the shoulder at 2.8 Å, the peak at 3.1 Å, and the other ripples of the experimental[38] $g_{NaO}(r)$. Since they are absent in the original $g_{NaO}(r)$, these features are all due to Fourier transform artifacts arising from the limited resolution, as previously suggested.[37] The height of the first peak and the overall distribution of intensity, instead, are not reproduced. The significance of this mismatch is difficult to assess, because the precision of the experiments is unknown. In fact, since the absence of suitable Na isotopes prevented the application of isotopic substitution methods, the X-ray $g_{NaO}(r)$ was obtained by substitution with Ag, which is not really isomorphic to Na.[38]

The self-diffusion coefficient D_{Na_+} of the Na^+ cation has been calculated by monitoring the mean squared displacement of the Na atoms as a function of time: $D = \langle[\boldsymbol{R}_{Na}(t) - \boldsymbol{R}_{Na}(0)]^2\rangle/6t$ (independent of t for large t). Since there is only a single Na atom in the simulation cell, we have improved the statistics by averaging over multiple time origins[62] 40 fs apart. For both the present and the AMBER models, the calculated diffusion coefficient is $D_{Na_+} = 2.8 \pm 0.1\ 10^{-5}$ cm^2/s. This is more than twice the experimental value,[63] $D_{Na_+} = 1.12\ 10^{-5}$ cm^2/s, but agrees with previous calculations[22] using the same combination of SPC[24,40] and Åqvist[43] models employed by AMBER. It has been noticed[22] that in diluted aqueous systems, where water molecules vastly outnumber the ions, the dynamics is determined by the water model while the effect of the ionic model is small. The diffusion constant is not a good indicator of the quality of the potential for sodium.

To summarize the results of the MD simulation on Na^+ in aqueous solution, the present model is at least as good as the AMBER model,[26] since it predicts comparable energies, radial correlation functions, and self-diffusion coefficients. All quantities, including the energies, are essentially size independent, as we have found by performing shorter simulations with a number of H_2O molecules ranging from 62 to 510 (and a corresponding box side L from 12.426 to 24.852 Å).

E. MD Simulation of Na^+(Phe) in Aqueous Solution. Once verified that the potential parameters describe correctly the Na^+(Phe) and $Na^+(H_2O)$ interactions, we have simulated a Na^+(Phe) complex in aqueous solution, as described in section IIIB. During the initial equilibration, several ns long, we have artificially maintained the ZW5 configuration[13] of the Na^+(Phe) complex by adding harmonic springs between the Na^+ and the carbons of the phenyl ring. At quite long intervals during this phase we have saved copies of the instantaneous state of the system, obtaining several uncorrelated initial configurations sampled from a canonical distribution. After severing the springs, these ZW5 configurations always survived for at least 0.2 ns, showing that Na^+(Phe) is bound even in water. The free energy barrier that must be overcome to detach the Na^+ cation from the complex, however, is not unsurmountable, since continuing the simulations eventually allowed the cation to break away, after 1.5 ns in the longest case. During these simulations we have separately recorded configurations in which the Na^+(Phe) remained bound and configurations in which the Na^+ carbons were far from the phenyl ring (distances $r_{NaC} > 6$ Å), for later comparison.

Since the simulations indicate that there is a barrier, we have analyzed the potential of mean force (PMF), determined by integrating the work performed during steered MD runs, as described in section IIIC. We sampled 16 paths, by using some of the previously mentioned uncorrelated ZW5 configurations as starting points of separate "forward" steered MD runs, in

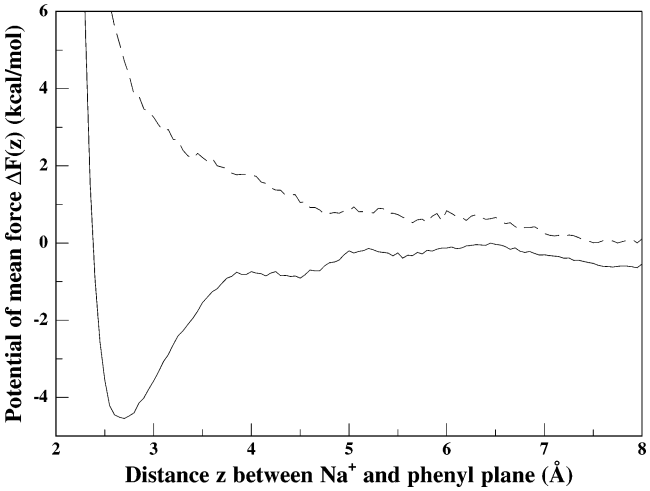

Figure 4. Potential of mean force $\Delta F(z)$ for Na^+(Phe) in aqueous solution as a function of the distance z between the Na^+ cation and the plane of the phenyl ring, calculated with the present model (solid line) and with the AMBER model[26] (broken line).

which z was continuously increased. The end point z_i^{max} of the ith forward run became the starting point of a corresponding "backward" run, in which z was decreased at the same speed. We thus obtained 16 pairs of PMF estimates $\Delta_i^{\pm} F(z)$, where the $\pm$ sign distinguishes between forward and backward runs. Since forward and backward runs share the state at the z_i^{max} end point, we impose $\Delta_i^{+}F(z_i^{max}) = \Delta_i^{-}F(z_i^{max})$ by appropriately shifting the origin of the free energy scale. The PMF averaged over all forward and backward runs, $\Delta F(z) = \overline{\Delta_i^{\pm}F(z)}$, is shown in Figure 4 as a function of the reaction coordinate z. The free energy barrier opposing dissociation of the solvated Na^+(Phe) complex is $\approx$ 4.5 kcal/mol, which is larger than, but still comparable to, the mean kinetic energy at 300 K, $3k_BT/2 \approx 0.9$ kcal/mol. The difference between the free energy barrier in aqueous solution and the corresponding energy barrier in vacuum (Table 1) is due to water solvation effects, which are very large.

The effects of non reversibility are small, since our data indicate that most of the work spent in going from a point z to z_i^{max} is reversibly recovered while returning to z. Averaging over all runs and all points z, we find $\sqrt{\overline{\Delta_i^{-}F(z) - \Delta_i^{+}F(z)}} = 0.5$ kcal/mol. The effects of the variety of paths are more significant, as we have discovered by examining the differences among the various $\Delta_i^{\pm}F(z)$ curves, which would all have the same shape if all runs follow the same path. After shifting all $\Delta_i^{\pm} F(z)$ functions to the same mean, we find a residual RMS dispersion of 3.5 kcal/mol.

It must be stressed that only the present model, which has been modified to describe the cation$-\pi$ interaction and the competition with water, predicts a bound Na^+(Phe) complex in aqueous solution. The PMF computed with the AMBER model,[26] also shown in Figure 4, does not exhibit a barrier. This difference between the two potential models is consistent with the results for the isolated Na^+(Phe) complex (Table 1). In the isolated complex the distances between Na^+ and the phenyl plane, $z \approx \sqrt{r_{NaC}{}^2 - r_{CC}{}^2}$, are 5.35 and 2.65 Å for the AMBER model and for the present model, respectively. The finding that for the AMBER model the PMF in aqueous solution is repulsive at least up to $z = 5$ Å, whereas for the present model there is a PMF minimum at $z \approx 2.70$ Å, is thus justified.

Interactions with the $-COO^-$ group contribute to the stability of the Na^+(Phe) complex, since the phenyl and the backbone containing the $-COO^-$ group always maintain their relative positions when the Na^+ cation is present. Furthermore, in some of the steered MD simulations, at the end of the backward run we have found the Na^+ cation attached on the phenyl face opposite to the $-COO^-$ group, showing that backbone and phenyl may change position while the cation is sufficiently far. The average free energy difference between backward runs ending with the ion attached on the $-COO^-$ side and runs ending on the opposite side is $\approx$ 1.5 kcal/mol, which represents the stabilization due to Na^+-COO^- interactions. We cannot estimate the corresponding uncertainty, due to insufficient statistics (three events only).

To better understand the solvation effects, we have analyzed the configurations recorded during the initial simulations, separately for bound and nonbound Na^+(Phe). We have thus determined the radial correlation functions for both types of configurations, $g_{ij}^{bound}(r)$ and $g_{ij}^{free}(r)$, and decomposed the total potential energy into Na^+-H_2O and Na^+-Phe binding, plus a remainder which includes all Phe$-H_2O$, H_2O-H_2O, and intramolecular interactions.

We have found that the computed differences $\overline{\Delta n_{ij}}$ in coordination numbers are much more accurate than the coordination numbers $\overline{n_{ij}}$ themselves. It is well known[62] that the number of atoms of species j contained in a spherical shell of radius r^{max} around a central atom of species i is proportional to $\int_0^{r_{max}} g_{ij}(r)\, 4\pi r^2\, dr$. Since the integral diverges as the cube of r^{max}, the number of neighbors $\overline{n_{ij}}$ is extremely sensitive to the choice of the cutoff radius. The difference in the number of neighbors $\overline{\Delta n_{ij}}$, instead, depends on the integral of $g_{ij}^{bound}(r) - g_{ij}^{free}(r)$, which is different from zero only at short distances, in the region where the two $g_{ij}(r)$ functions are different. In this case the integral is well behaved and weakly sensitive to the cutoff radius. We find few differences between the atomic coordination numbers, going from independently solvated Na^+ and Phe to a bound Na^+(Phe) complex in water. The Na^+ cation sheds two H_2O neighbors and becomes coordinated to the phenyl ring, displacing a single H_2O molecule, and to the $-COO^-$ moiety, displacing another H_2O molecule. No other significant differences are noticeable.

The redistribution of the various potential energy contributions during the binding process follows the adjustments in the number of neighbors. The Na^+-H_2O potential energy goes from -99 to -70 kcal/mol. These values are consistent with the $Na^+(H_2O)_n$ binding energies (Table 1) with $n = 6$ or 4, respectively, if one allows for disorder and for the binding with water molecules beyond the first solvation shell. The binding energy for freely solvated Na^+ also matches the range of 102$-$104 kcal/mol reported[64] for the experimental solvation enthalpy. The energy expended to detach the two H_2O molecules from the Na^+ cation, while forming the solvated Na^+(Phe) complex, is more than compensated by the gain in Na^+-Phe binding, -31 kcal/mol, which is nearly as strong as the binding of the isolated Na^+(Phe) complex (Table 1). Finally, the remaining Phe$-H_2O$ and H_2O-H_2O interactions, which fluctuate quite wildly, on the average yield a further additional stabilization of a few kcal/mol.

V. Concluding Remarks

In the present paper, we report the main results of a comprehensive investigation on the competition between aqueous solvation and cation$-\pi$ interaction for the Na^+(Phe) (Na^+-phenylalanine) complex. In a first step, we tested the AMBER[26] force field, which has been identified[15] as one of

the best standard potential models. Since the test was not fully satisfactory, we modified some potential parameters to obtain reliable structures and binding energies for a number of small complexes, including Na^+(Phe), $Na^+(C_6H_6)$, and $Na^+(H_2O)_n$ with n up to 6, for which experimental binding energies and refined quantum mechanical computations are available. It is noteworthy that just slight modifications (essentially relaxing the arithmetic mixing rules for some nonbonded parameters involving the Na^+ cation) are sufficient to obtain an excellent agreement with the reference results, as well as good results for Na^+ in aqueous solution. Next, a number of MD simulations have been performed with the modified force field, to investigate the stability of the Na^+(Phe) complex in aqueous solution.

We have found that the so-called ZW5 structure,[13] in which phenylalanine assumes a zwitterionic structure with $-COO^-$ and $-NH_3^+$ ends and the Na^+ ion interacts with both $-COO^-$ and phenyl groups, survives for a significant time in aqueous solution. By performing a thermodynamic integration during steered MD simulations,[55,56] we have then determined the potential of mean force as a function of the distance z between the Na^+ cation and the plane of the phenyl ring. We have thus confirmed, from a quantitative point of view, that there is a significant free energy barrier opposing dissociation of the Na^+(Phe) complex. Finally, we have analyzed the role of the various interactions in determining the preference for the ZW5 structure of the Na^+(Phe) complex in water.

Acknowledgment. Work done with funds from MIUR (PRIN project and FIRB project through INSTM consortium). We thank P. Procacci for support with the ORAC program, D. Feller, E. D. Glendening, D. E. Woon and M. W. Feyereisen for providing their QM structures, and the CINECA Supercomputer Center for an allocation of computer resources. We thank G. W. Neilson and N. T. Skipper for information on the experimental radial correlation function.

References and Notes

(1) Dougherty, D. A.; Stauffer, D. A. *Science* **1990**, *250*, 1558−1560.
(2) Dougherty, D. A. *Science* **1996**, *271*, 163.
(3) Ma, J. C.; Dougherty, D. A. *Chem. Rev.* **1997**, *97*, 1303−1324.
(4) Armentrout, P. B.; Rodgers, M. T. *J. Phys. Chem. A* **2000**, *104*, 2238−2247.
(5) Džidic, I.; Kebarle, P. *J. Phys. Chem.* **1970**, *74*, 1466−1474.
(6) Guo, B. C.; Purnell, J. W.; Castleman, A. W., Jr. *Chem. Phys. Lett.* **1990**, *168*, 155.
(7) Kish, M. M.; Ohanessian, G.; Wesdemiotis, C. *Int. J. Mass Spectrosc.* **2003**, *227*, 509.
(8) Gapeev, A.; Dunbar, R. C. *J. Am. Chem. Soc.* **2001**, *123*, 8360−8365.
(9) Gapeev, A.; Dunbar, R. C. *Int. J. Mass Spectrom.* **2003**, *228*, 825.
(10) Ryzhov, V.; Dunbar, R. *J. Am. Soc. Mass Spectrom.* **2000**, *11*, 1037.
(11) Ruan, C.; Rodgers, M. T. *J. Am. Chem. Soc.* **2004**, *126*, 14600.
(12) Dunbar, R. C. *J. Phys. Chem. A* **2000**, *104*, 8067.
(13) Siu, F. M.; Ma, N. L.; Tsang, C. W. *J. Am. Chem. Soc.* **2001**, *123*, 3397−3398; energies and structures are available at the Journal Web site.
(14) Meyer, E. A.; Castellano, R. K.; Diederich, F. *Angew. Chem., Int. Ed.* **2003**, *42*, 1210.
(15) Minoux, H.; Chipot, C. *J. Am. Chem. Soc.* **1999**, *121*, 10366−10372.
(16) Gallivan, J. P.; Dougherty, D. A. *Proc. Natl. Acad. Sci. U.S.A.* **1999**, *96*, 9459−9464.
(17) Gallivan, J. P.; Dougherty, D. A. *J. Am. Chem. Soc.* **2000**, *122*, 870−874.
(18) Meadows, E. S.; De Wall, S. L.; Barbour, L. J.; Gokel, G. W. *J. Am. Chem. Soc.* **2001**, *123*, 3092−3107.
(19) Hu, J.; Barbour, L. J.; Gokel, G. W. *Proc. Natl. Acad. Sci. U.S.A.* **2002**, *99*, 5121.
(20) Siu, F. M.; Ma, N. L.; Tsang, C. W. *Chem. Eur. J.* **2004**, *10*, 1966−1976.
(21) Guillot, B. *J. Mol. Liq.* **2002**, *101*, 219−260.
(22) Patra, M.; Karttunen, M. *J. Comput. Chem.* **2004**, *25*, 678−689.
(23) Mu, Y. G.; Kosov, D. S.; Stock, G. *J. Phys. Chem. B* **2003**, *107*, 5064−5073.
(24) Berendsen, H. J. C.; Grigera, J. R.; Straatsma, T. P. *J. Phys. Chem.* **1987**, *91*, 6269−6271.
(25) Cornell, W. D.; Cieplak, P.; Bayly, C. I.; Kollmann, P. A. *J. Am. Chem. Soc.* **1993**, *115*, 9620−9631.
(26) Cornell, W. D.; Cieplak, P.; Bayly, C. I.; Gould, I. R.; Merz, K. M., Jr.; Ferguson, D. M.; Spellmeyer, D. C.; Fox, T.; Caldwell, J. W.; Kollman, P. A. *J. Am. Chem. Soc.* **1995**, *117*, 5179−5197.
(27) Chipot, C.; Maigret, B.; Pearlman, D. A.; Kollman, P. A. *J. Am. Chem. Soc.* **1996**, *118*, 2998−3005.
(28) Caldwell, J. W.; Kollman, P. A. *J. Am. Chem. Soc.* **1995**, *117*, 4177.
(29) Tsuzuki, S.; Yoshida, M.; Uchimaru, T.; Mikami, M. *J. Phys. Chem. A* **2001**, *105*, 769−773.
(30) Cubero, E.; Luque, F. J.; Orozco, M. *Proc. Natl. Acad. Sci. U.S.A.* **1998**, *95*, 5976−5980.
(31) Mecozzi, S.; West, A. P. Jr.; Dougherty, D. A. *J. Am. Chem. Soc.* **1996**, *118*, 2307−2308.
(32) Kraulis, P. J. *J. Appl. Crystallogr.* **1991**, *24*, 946.
(33) Berg, J. M.; Tymoczko, J. L.; Stryer, L. *Biochemistry*; W. H. Freeman and Co.: New York, 2001.
(34) Hoyau, S.; Norrman, K.; McMahon, T. B.; Ohanessian, G. *J. Am. Chem. Soc.* **1999**, *121*, 8864−8875.
(35) Feller, D.; Glendening, E. D.; Woon, Feyereisen, D. E. M. W. *J. Chem. Phys.* **1995**, *103*, 3825.
(36) Feller, D. *Chem. Phys. Lett.* **2000**, *322*, 543−548.
(37) White, J. A.; Schwegler, E.; Galli, G.; Gygi, F. *J. Chem. Phys.* **2000**, *113*, 4668.
(38) Skipper, N. T.; Neilson, G. W. *J. Phys.: Condens. Matter* **1989**, *1*, 4141−4154.
(39) Caminiti, R.; Licheri, G.; Paschina, G.; Piccaluga, G.; Pinna, G. *J. Chem. Phys.* **1980**, *72*, 4522−4528.
(40) Straatsma, T. P.; Berendsen, H. J. C. *J. Chem. Phys.* **1988**, *89*, 5876−5886.
(41) Gervasio, F. L.; Chelli, R.; Marchi, M.; Procacci, P.; Schettino, V. *J. Phys. Chem. B* **2001**, *105*, 7835−7846.
(42) Procacci, P.; Darden, T. A.; Paci, E.; Marchi, M. *J. Comput. Chem.* **1997**, *18*, 1848−1862; http://www.chim.unifi.it/orac/.
(43) Aqvist, J. *J. Phys. Chem.* **1990**, *94*, 8021.
(44) Becke, A. D. *Phys. Rev. A* **1988**, *38*, 3098−3100.
(45) Lee, C.; Yang, W.; Parr, R. G. *Phys. Rev. B* **1988**, *37*, 785−789.
(46) Frisch, M. J.; Trucks, G. W.; Schlegel, H. B.; Scuseria, G. E.; Robb, M. A.; Cheeseman, J. R.; Zakrzewski, V. G.; Montgomery, J. A., Jr.; Stratmann, R. E.; Burant, J. C.; Dapprich, S.; Millam, J. M.; Daniels, A. D.; Kudin, K. N.; Strain, M. C.; Farkas, O.; Tomasi, J.; Barone, V.; Cossi, M.; Cammi, R.; Mennucci, B.; Pomelli, C.; Adamo, C.; Clifford, S.; Ochterski, J.; Petersson, G. A.; Ayala, P. Y.; Cui, Q.; Morokuma, K.; Malick, D. K.; Rabuck, A. D.; Raghavachari, K.; Foresman, J. B.; Cioslowski, J.; Ortiz, J. V.; Stefanov, B. B.; Liu, G.; Liashenko, A.; Piskorz, P.; Komaromi, I.; Gomperts, R.; Martin, R. L.; Fox, D. J.; Keith, T.; Al-Laham, M. A.; Peng, C. Y.; Nanayakkara, A.; Gonzalez, C.; Challacombe, M.; Gill, P. M. W.; Johnson, B. G.; Chen, W.; Wong, M. W.; Andres, J. L.; Head-Gordon, M.; Replogle, E. S.; Pople, J. A. *Gaussian 98*, revision A.5; Gaussian, Inc.: Pittsburgh, PA, 1998.
(47) Garau, C.; Frontera, A.; Quinonero, D.; Ballester, P.; Costa, A.; Deya, P. M. *Chem. Phys. Lett.* **2004**, *392*, 85−89.
(48) Nosé, S. *J. Chem. Phys.* **1984**, *81*, 511.
(49) *CRC Handbook of Chemistry and Physics*, 84-th edition; CRC Press: Boca Raton 2003.
(50) Essmann, U.; Perera, L.; Berkowitz, M. L.; Darden, T.; Lee, H.; Pedersen, L. G. *J. Chem. Phys.* **1995**, *103*, 8577.
(51) Woodcock, L. V.; Singer, K. *Trans. Faraday Soc.* **1971**, *67*, 12.
(52) Tuckerman, M.; Berne, B. J.; Martyna, G. J. *J. Chem. Phys.* **1992**, *97*, 1990.
(53) Procacci, P.; Berne, B. J. *J. Chem. Phys.* **1994**, *101*, 2421.
(54) Marchi, M.; Procacci, P. *J. Chem. Phys.* **1998**, *109*, 5194.
(55) Park, S.; Khalili-Araghi, F.; Tajkhorshid, E.; Schulten, K. *J. Chem. Phys.* **2003**, *119*, 3559−3566.
(56) Park, S.; Schulten, K. *J. Chem. Phys.* **2004**, *120*, 5946−5961.
(57) Jarzynski, C. *Phys. Rev. Lett.* **1997**, *78*, 2690−2693.
(58) Hummer, G. *J. Chem. Phys.* **2001**, *114*, 7330−7337.
(59) Lukyanov, S. I.; Zidi, Z. S.; Shevkunov, S. V. *J. Mol. Struct. Theochem* **2003**, *623*, 221−236.
(60) Laio, A.; VandeVondele, J.; Rothlisberger, U. *J. Phys. Chem. B* **2002**, *106*, 7300−7307.
(61) Hartke, B.; Charvat, A.; Reich, M.; Abel, B. *J. Chem. Phys.* **2002**, *116*, 3588.
(62) Allen, M. P.; Tildesley, D. J. *Computer Simulation of Liquids*; Clarendon: Oxford, 1987.
(63) Ohtaki, H.; Radnai, T. *Chem. Rev.* **1993**, *93*, 1157−1204.
(64) Lybrand, T. P.; Kollman, P. A. *J. Chem. Phys.* **1985**, *83*, 2923−2933.